

# Topology Optimized Microbioreactors

Daniel Schapper,<sup>1</sup> Rita Lencastre Fernandes,<sup>1</sup> Anna Eliasson Lantz,<sup>2</sup> Fridolin Okkels,<sup>3</sup> Henrik Bruus,<sup>1</sup> Krist V. Gernaey<sup>1</sup>

<sup>1</sup>Department of Chemical and Biochemical Engineering, Technical University of Denmark, Søltofts Plads, Building 229, 2800 Kgs. Lyngby, Denmark; telephone: +45-2011-5827; fax: +45-4593-2906; e-mail: daniel.schaepper@schappi.dk

<sup>2</sup>Department of Systems Biology, Technical University of Denmark, Kgs. Lyngby, Denmark

<sup>3</sup>Department of Micro- and Nanotechnology, Technical University of Denmark, Kgs. Lyngby, Denmark

Received 1 July 2010; revision received 7 October 2010; accepted 20 October 2010

Published online 12 November 2010 in Wiley Online Library (wileyonlinelibrary.com). DOI 10.1002/bit.23001

**ABSTRACT:** This article presents the fusion of two hitherto unrelated fields—microbioreactors and topology optimization. The basis for this study is a rectangular microbioreactor with homogeneously distributed immobilized brewers yeast cells (*Saccharomyces cerevisiae*) that produce a recombinant protein. Topology optimization is then used to change the spatial distribution of cells in the reactor in order to optimize for maximal product flow out of the reactor. This distribution accounts for potentially negative effects of, for example, by-product inhibition. We show that the theoretical improvement in productivity is at least fivefold compared with the homogeneous reactor. The improvements obtained by applying topology optimization are largest where either nutrition is scarce or inhibition effects are pronounced.

Biotechnol. Bioeng. 2011;108: 786–796.

© 2010 Wiley Periodicals, Inc.

**KEYWORDS:** microbioreactor; topology optimization; yeast; productivity

## Introduction

In bioprocesses for industrial applications, genetically engineered microorganisms are used for the production of cell products of commercial interest, for example, enzymes or antibiotics. A part of the bioprocess design is then concerned with *optimizing the growth* of a chosen strain according to criteria such as productivity, outlet product concentration or substrate conversion efficiency. This optimization is normally done by adjusting process variables such as temperature or pH, by adjusting the feed profile or by modifying the strain. Another aspect of bioprocess design is concerned with *reactor design*, where focus is on obtaining sufficient agitation and aeration to overcome mass transfer limitations which decrease productivity and yield.

Correspondence to: D. Schapper

Contract grant sponsor: Novozymes A/S

There has recently been considerable interest in the development of microbioreactors (volume below 1 mL) that allow experimentation with microorganisms at microscale under well-controlled conditions (Lee et al., 2006; Schapper et al., 2009, 2010; Szita et al., 2005; Zhang et al., 2007). When performing fermentation experiments at microscale, the increased design flexibility offered by the microfluidic systems enables a wide range of reactor configurations, potentially leading to higher productivities compared to traditional reactor designs. In fact, the incorporation of solid structures in the microreactor, resulting in a more complex flow pattern, has been shown to result in a significant metabolic rate increase for a simplified model of a bio-process (Okkels and Bruus, 2007b).

In this article, a new approach in designing the microbioreactor layout is taken by the introduction of *topology optimization*. This combined mathematical optimization technique and simulation tool allows for the determination of the optimal distribution of (reactor) design structures and thus improves the engineering design process. The methodology was first applied to the field of structural mechanics (Bendsøe and Kikuchi, 1988; Bendsøe and Sigmund, 2002), and has been recently implemented to the field of microfluidic systems (Borrvall and Petersson, 2003; Gregersen et al., 2009; Højgaard-Olesen et al., 2006). Further the method has been successfully applied to the design of optimal catalytic microreactors (Okkels and Bruus, 2007a), which are very analogous to simplified models of microbioreactors.

Topology optimization puts the traditional design process upside down: Instead of letting the ingenuity of the engineer guide the change of the structural design to achieve the best results, the engineer now formulates the problem, implements it in an iterative computer code, and then lets the computer find an optimal solution. Subsequently, the engineer may have to simplify the computer-generated design such that it can be fabricated and is economically

viable. A wealth of methodologies for topology optimization has emerged (Eschenauer and Olhoff, 2001; Bendsoe et al., 2005). Common for all these numerical methods is that they iteratively optimize the given system according to the value of a certain pre-defined objective function (e.g. maximum mechanical strength of a bridge or maximal production rate of a product in a biological system) and constraints (e.g. an upper limit of the amount of material to be used for building a bridge or a maximum concentration of a toxic byproduct in the reactor). The main advantage of the method is that it relies on the user-specified governing equations and constraints, and not on any a priori assumptions regarding the geometry of the structure. Often, as is also the case in this study, the structural solutions found by topology optimization are unexpected and better than conventional structures.

In the present work we study microbioreactors optimized for maximal local production rate (the goal function) of a certain soluble recombinant protein by an immobilized microorganism, the spatial distribution (design field) of which is found by topology optimization. To the best of our knowledge, this is the first time topology optimization is applied in combination with a biological model describing nonlinear microbial kinetics in a biological case study, and therefore we want to answer the following main question: Is it possible to significantly improve the performance of a conventional reactor with homogeneously distributed immobilized biomass, by letting topology optimization change the spatial distribution of the immobilized biomass keeping all other parameters fixed?

In the following we first present the motivation for this work and discuss possible gains to be expected from a structurally optimized reactor. The topology optimization methodology is then explained in more detail followed by a description of the original biological model and its adaptation to the topology optimization routine. The simulated reactor layouts are then presented and their performance is compared to a benchmark. Finally, we give an outlook over the possibilities and challenges presented by this combination of technologies.

## Modeling and Optimization

There is a constant need for both strain and process improvement within the biotechnology industry to maintain competitiveness. In this context, mechanistic models describing the different phenomena taking place in the (bio)reactor are important tools for optimization and control of the process (Gernaey et al., 2010). The interplay between different metabolic pathways, regulation mechanisms, inhibition by substrates and products, and formation of intermediate substrates and products results in complex kinetic models. When it comes to modeling of the mass flow, the commonly used stirred tank bioreactors are most often assumed as ideal, and thus the existence of concentration gradients throughout the reactor is neglected. However, in large scale production bioreactors concentration gradients

of substrates and products do exist as demonstrated by experimental work in combination with computational fluid dynamics (CFD) and may have a significant influence on the resulting yields and productivities of a process (Enfors et al., 2001; Lapin et al., 2004).

For systems with immobilized cells, topology optimization might allow for higher productivities by optimizing the spatial distribution of the immobilized microorganisms within the reactor (and thus controlling and optimizing the concentration gradients present in the reactor). This might, at least hypothetically, minimize the negative effects on the process due to lack of substrate or excessive amounts of substrate (substrate inhibition), or accumulation of a metabolite or a product (product inhibition).

Our model for optimizing the distribution of cells immobilized onto a carrier within a microbioreactor consists of three parts: One part is the modeling of the flow of the culture broth (consisting of culture medium and suspended cells) and how it is affected by the presence of solid structures such as walls and immobilized cells. Another part is the modeling of the reaction kinetics of cell growth, substrate consumption, and product formation. The third and final part is the iteration procedure involving the evaluation of system performance combined with sensitivity analysis to determine the incremental change in the immobilized cell distribution in each iteration step leading towards optimality.

## Fluid Dynamic Modeling of the Flow

Driven by a steady pressure field  $p$  [Pa], the broth perfuses with a flow velocity  $\bar{u}$  [ $\text{m s}^{-1}$ ] through the microreactor containing carrier and immobilized cells. The broth has density  $\rho$  [ $\text{kg m}^{-3}$ ] and viscosity  $\eta$  [Pa s], and hydrodynamically the presence of the cells and the carrier in the reactor is modeled as a porous, sponge-like material. This gives rise to an additional friction in the flow of the broth, the so-called Darcy friction  $-\alpha\bar{u}$ , which is anti-parallel and proportional to the velocity. The porous material may be inhomogeneously distributed, so in general the friction coefficient  $\alpha$  depends on position (Borrvall and Petersson, 2003; Højgaard-Olesen et al., 2006). If at some point  $\bar{r}_0$  in space no cells are present then  $\alpha(\bar{r}_0) = 0$ , and the broth flow is unhindered at that point, while a large and dense concentration of cells results in a high value of  $\alpha$ , typically in the range of  $10^5$  to  $10^8$  [ $\text{Pa s m}^2$ ], and thus a high flow resistance. Mathematically, the broth velocity  $\bar{u}$  can be calculated from the steady-state Navier–Stokes equation, including the Darcy friction of the porous material

$$\rho(\bar{u}\nabla)\bar{u} = -\nabla p + \eta\nabla^2\bar{u} - \alpha(\bar{r})\bar{u} \quad (1)$$

and from the incompressibility condition for the broth

$$\nabla\bar{u} = 0 \quad (2)$$

## Topology Optimization: Objective Function $\Phi$ and Design Field $\gamma$

Contrary to conventional numerical design processes, the final geometrical structure is not known in topology optimization problems. Instead, starting from an arbitrary initial structure, it gradually forms through an iterative optimization process within a design region, denoted  $\Omega$ . To guide the optimization process, the value of a pre-defined objective function  $\Phi$  is calculated for each candidate geometry generated during the iteration, and gradual geometrical changes are made for each iteration step to optimize (by convention minimize)  $\Phi$  until convergence (global minimization) is reached.  $\Phi$  can depend on any aspect of a given candidate geometry, such as structure and performance, and to choose a proper objective function among the many possible ones is generally not easy and constitutes a major step in establishing a successful topology optimization procedure.

To facilitate the optimization procedure each candidate geometry is uniquely parameterized by a set of so-called design variables  $\gamma$  ranging from zero to unity. This might, for example, denote the densities of the structure at the various points in the design space and would thus parameterize the material distribution. Every set of design variables is unique in the sense that for each set there exists a unique solution of the model system which in turn can be evaluated by the objective function  $\Phi$  (Bendsøe and Sigmund, 2002). A different set of design variables leads to a different geometry and a corresponding distinct solution which may or may not be equal to the solution of another design variable set. In our case we use as design field  $\gamma(\bar{r})$  the local volume fraction occupied by the liquid cultivation broth at the position  $\bar{r}$  (Desmet et al., 2003). For the minimum value  $\gamma=0$  no broth is present due to a maximal occupancy of carrier with immobilized cells (porous structure), while for the maximum value  $\gamma=1$  only broth is present (open channel). The geometrical structure is fully determined by the design field  $\gamma(\bar{r})$ , which by the end of a successful iterative topology optimization procedure only takes the values zero (regions filled with porous carrier) and unity (regions of open channels), with no regions having intermediate values. The Darcy friction coefficient  $\alpha(\bar{r})$  in Equation (1) depends linearly on the design field  $\gamma(\bar{r})$

$$\alpha(\bar{r}) = \alpha_{\max}(1-\gamma(\bar{r})) \quad (3)$$

where  $\alpha_{\max}$  is the maximum value of the inverse permeability of the broth flow inside the porous structure as described above. For simple flow problems, this linear correlation turns out to ensure a sharp transition in space between buffer regions and solid or densely porous material regions (Borrvall and Petersson, 2003). This property was observed to hold for the optimized solutions of many simple reactor models (Okkels and Bruus, 2007a).

In the present model, the distributed material is assumed to be a dense porous carrier with immobilized cells, which consume substrate in order to grow and produce a

soluble recombinant protein. We have found that a suitable objective function is (minus) the total production rate which is the integral of the local product formation rate  $R_p(t)$  [ $\text{kg s}^{-1}$ ] (defined in Eq. A.10) specified for every point in the reactor  $\Omega$

$$\Phi(\gamma) = - \int_{\Omega} R_p(t) dV \quad (4)$$

where the minus sign is introduced to follow the convention that the objective function should be minimized.

Besides defining an objective function  $\Phi(\gamma)$  in optimization problems, additional constraints on the design variable  $\gamma$  or on other variables of the system often have to be defined to avoid non-physical or trivial solutions to the problem. However, this is not the case in this work as the extreme cases of a completely full or completely empty reactor are unfavorable. In the first case the material will act as a plug, blocking the pressure-driven flow, and only a minimal amount of end-product will leave through the outlet channel, while the absence of active material in the second case naturally will be worse, as no reaction will happen at all.

Only for very few ideal systems, it can be proven that the obtained solution is globally optimal; however, it is easily tested how much of an improvement it represents (Bendsøe and Sigmund, 2002; Borrvall and Petersson, 2003; Gregersen et al., 2009).

## Implementation of the Biological Model

Heterologous protein production by the yeast *Saccharomyces cerevisiae* was chosen for this study as it is one of the best-known model systems and because *S. cerevisiae* is one of the microorganisms most commonly used in the biotech industry. Its production of the protein will be negatively affected by, for example, too high substrate concentration which makes spatial optimization interesting. Although typical yeast cultivations consist of suspended cells, yeast can also grow adsorbed onto a carrier (immobilization support) which thus allows for a varying spatial distribution of cells. This has been exploited in biotechnological processes offering advantages such as increased process flow rates (Brányik et al., 2004).

In the system presented here, the cells are both attached onto a carrier and freely suspended in the culture medium. The dynamics of immobilization of brewing yeast cells by adsorption onto a carrier (spent grain particles) have earlier been modeled by Brányik et al. (2004).

In this model a certain fraction of the yeast cells was assumed to possess a plasmid which encodes for a recombinant protein, the product we aimed to obtain from the cultivation (Zhang et al., 1997). Glucose was fed to the reactor, and was assumed to be the preferred substrate. The yeast metabolism was simplified to a three-pathway model suggested by Zhang et al. (1997). A new model (schematically presented in Fig. 1, equations provided in Appendix

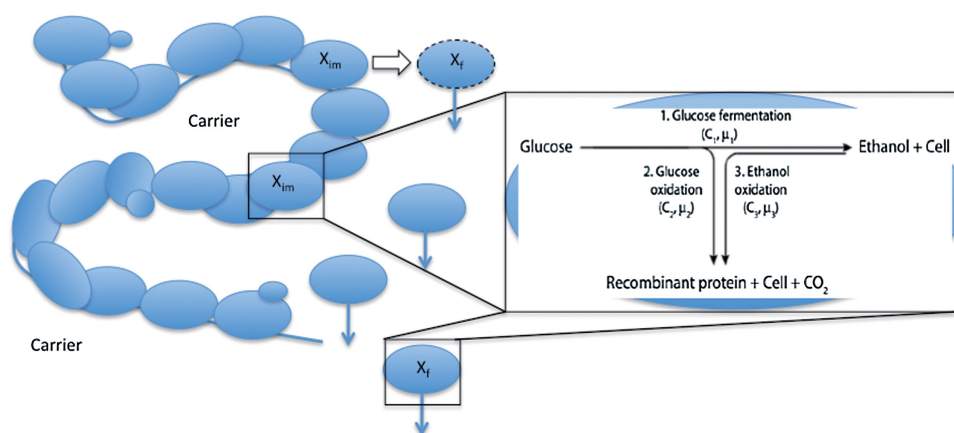


**Figure 1.** The new model combining the model for dynamics of the immobilization of brewing yeast cells (Brányik et al., 2004) and the three-pathway model for the yeast metabolism where  $C_i$  is a pool of enzymes and  $\mu_i$  is the specific growth rate (Zhang et al., 1997). [Color figure can be seen in the online version of this article, available at <http://wileyonlinelibrary.com/bit>]

1), based both on the work of Brányik et al. (2004) and Zhang et al. (1997), was required in order to perform the topology optimization. The purpose of the new model is to simulate a cultivation in a microbioreactor where brewing yeast, both immobilized onto a support (carrier) and suspended in the cultivation medium, grows, and produces an extracellular soluble recombinant protein P, which is encoded in a plasmid.

### Growth Kinetics

The model describes three metabolic events (Fig. 1): glucose fermentation, glucose oxidation, and ethanol oxidation. Under aerobic conditions, glucose is oxidized to carbon dioxide along the respiratory metabolic pathways. However, if the glucose flow becomes too large for the respiratory capacity of the cell, excess glucose is fermented to ethanol and the activity of the enzymes in the glucose oxidation pathway is reduced. This phenomenon is typically referred to as the Crabtree effect and is schematically represented by pathways 1 and 2. When glucose approaches depletion, ethanol begins to be metabolized by pathway 3 in the presence of oxygen. The cells grow exclusively on ethanol when glucose is exhausted.

The recombinant protein production is connected to growth and is exclusively associated to the oxidative metabolism (pathways 2 and 3) in yeast cells (suspended or immobilized) carrying the plasmid. The fraction of plasmid bearing cells of the total immobilized cell population, which was set manually, was assumed to be constant.

Additionally, the three pathways were considered quantitatively additive, and were described by modified Monod equations, Equations (5)–(7). Although formulated differently, the proposed expressions for growth rates are mathematically equivalent to the implicitly defined functions proposed by Zhang et al. (1997). The use of explicit

and continuous functions, rather than implicit, step-change equations, is required in order to integrate this metabolism model into a topology optimization routine. In comparison to the original model proposed by Zhang et al. (1997), a third simplification was introduced: It was assumed that the consumption of substrate for microorganism maintenance was negligible; thus the maintenance coefficient in the model becomes zero. This assumption can safely be taken as only about 5% of the total glucose consumption goes to maintenance (Brányik et al., 2004). It can be assumed that the inclusion of the maintenance coefficient would lead to an increased glucose demand which again would lead to finer structures in the reactor.

$$\mu_1 = \mu_{1,\max} \frac{G}{K_{1'} + G} \frac{1 + k_{a'}G}{k_{b'} + k_{a'}G} \quad (5)$$

$$\mu_2 = \mu_{2,\max} \frac{G}{K_{2'} + G} \frac{1 + k_{c'}G}{1 + k_{c'}k_{d'}G} \quad (6)$$

$$\mu_3 = \mu_{3,\max} \frac{E}{K_3 + E} (1 - \tanh(G)) \quad (7)$$

### Immobilization Kinetics

Cells can attach onto and detach from the immobilization support (carrier). Brányik et al. (2004) have argued that the deposition rate is proportional to the dilution rate and the detachment rate is a function of the glucose concentration. As mentioned previously, the calculations concerning the flow of the liquid cultivation medium are performed separately from the ones concerning cell metabolism—thus a dilution rate dependent term describing the deposition of cells onto the carrier is problematic. However, as the deposition coefficient determined by Brányik et al. (2004)

was of a considerably lower order of magnitude than the detachment and growth rates, the deposition was disregarded in the formulation of the new model. In order to keep the amount of immobilized cells constant for the duration of one simulation, the growth rate of the immobilized cells was set equal to the detachment rate. If this was not the case, then the amount of immobilized biomass could change during the duration of one simulation which conflicts with the fact that the distribution of immobilized biomass is the very optimization parameter itself that is being used by the routine. In short, the optimization routine would no longer be able to control the amount of immobilized biomass. Therefore, the distribution of immobilized biomass is kept constant for one calculation run. In addition, it was assumed that only a constant fraction of the immobilized biomass,  $X_{im}^{act}$ , is actively growing, as observed experimentally by Brányik et al. (2004).

Concerning the release of cells from the support as a result of the flow of the culture broth, the detachment kinetics is mathematically described by Equation (8), where  $C_3$  reflects a switch to growth on ethanol (pathway 3) caused by glucose depletion. It was assumed that the saturation constant  $K_s$  was the same for both substrates (glucose and ethanol).

$$k_{det}^* = k_{det}^{sst} \frac{G}{G + K_s} + C_3 \frac{E}{E + K_s} \quad (8)$$

### Model for Topology Optimization: Spatial Dependency

In typical bioprocess models for continuously stirred reactors (CSTR), the reactors are assumed to be perfectly mixed (even though they are not, as observed, e.g., by Müller et al., 2010), and therefore, the state variables are not dependent of their location within the reactor. However, due to the heterogeneity in the optimized microreactor space resulting from the inhomogeneous distribution of immobilized cells and the linear flow regime, spatial dependency now has to be taken into account. In this case, the reactor can be considered to be a collection of local, infinitesimally small CSTRs, where transport across the interfaces is described by diffusion, and the fluid transport in the reactor is described by convection. In essence, the model reduces the size of the CSTRs to a limited number of cells each which all experience the exact same conditions.

Assuming steady-state conditions at each position, the total variation of a general state variable  $A$  is given by Equation (9) where  $\bar{u}$  represents the velocity vector [ $m s^{-1}$ ] and  $D_A$  [ $m^2 s^{-1}$ ] is the diffusion coefficient for the variable  $A$ . Similar equations were written for the following model state variables: glucose concentration  $G$  [ $g L^{-1}$ ], ethanol concentration  $E$  [ $g L^{-1}$ ], total free (suspended) biomass  $X_f$  [ $g L^{-1}$ ], plasmid bearing freely suspended biomass  $X_f^+$  [ $g L^{-1}$ ], and protein concentration  $P$  [ $U L^{-1}$ ].

$$\bar{u} \nabla A = \text{Sources} - \text{Sinks} + D_A \nabla^2 A \quad (9)$$

It is important to note that the terms *Sources* and *Sinks* in Equation (9) stand for the production or the consumption of the given component but do not include any terms related to the transport into or out from the infinitesimally small reactors, as these are accounted for in the convective term on the left hand side of Equation (9). These convective terms are taken care of by the CFD calculations for the flow of the culture broth that is considered to be a one-phase flow (liquid only). The cells in suspension are assumed not to significantly influence the flow characteristics of the liquid. Consequently, when referring to the suspended biomass, the sources are the detachment of immobilized cells, as well as the growth of the suspended population. As cell deposition is disregarded, there are no sinks for suspended biomass. In the case of the glucose substrate, there are no sources to be considered, whereas the sinks are the consumption of glucose by immobilized and suspended cells for both glucose oxidation and glucose fermentation. Finally, with regard to ethanol, the sources are the production of this component by glucose fermentation and the sink corresponds to the ethanol consumption by the ethanol oxidation pathway. The corresponding equations are all presented in Appendix 1.

As the immobilized biomass is not transported, different considerations have to be made for the variables  $X_{im}$  and  $X_{im}^+$ . The former can be called an actuator variable, as it is imposed in the beginning of each iteration of the optimization routine when the distribution of the carrier material (and with it the distribution of the immobilized cells) is determined, and the other state variables are calculated based on it. The latter,  $X_{im}^+$ , is directly proportional to  $X_{im}$  as the fraction of plasmid bearing cells in the immobilized population is assumed to be constant.

Thus, in summary, the overall optimization procedure (Fig. 2) is such that:

- (1) A certain initial distribution of carrier material and immobilized cells is assumed. Most often the initial assumption is that biomass is just homogeneously distributed, but in theory the starting point for the optimization can also be a completely different situation.
- (2) The steady-state flow of the culture broth (liquid with suspended cells) through the structure is calculated. This, for example, defines how much glucose moves from one infinitesimally small CSTR to the other.
- (3) Based on these results the cell kinetic model is run. The results here are, for example, the product concentrations in every small CSTR.
- (4) The optimization procedure determines if the solution is good enough, that is, if the stop criterion for the optimization is fulfilled. If it is not, a new direction (resulting in a new distribution of material) is determined.
- (5) The process restarts at step (1) and runs until the resulting solution fulfills the stop criterion for the optimization.

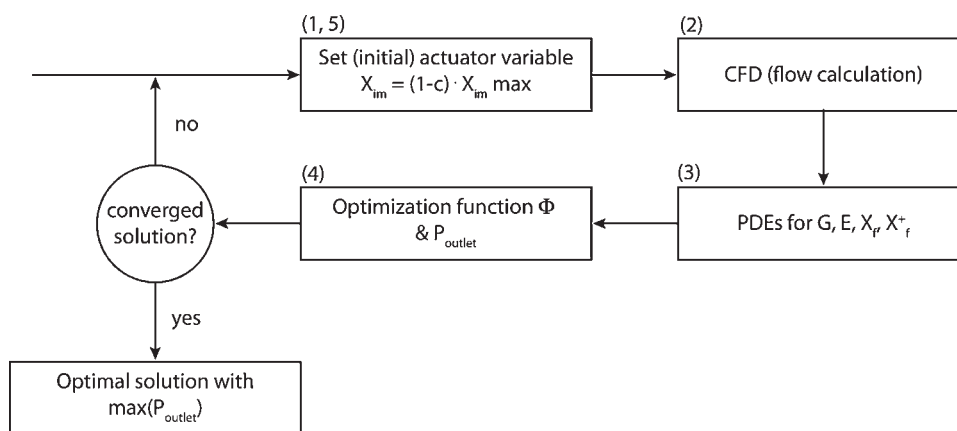


**Figure 2.** Scheme depicting the optimization procedure.

## Simulation Results

The topology optimization routine was implemented and solved using the commercially available software COMSOL (COMSOL A/S, Kgs. Lyngby, Denmark) coupled with MATLAB (The MathWorks, Inc., Natick, MA, USA). Simulations were carried out for a rectangular microbioreactor of length 1.2 mm, width 1.2 mm, and height 1 mm. Although the reactor height was taken into account in the calculation of the viscous friction of the flow, it was assumed that the flow is two-dimensional. Therefore, the state variables were considered constant along the  $z$ -axis and vary only along the  $x$ - and  $y$ -axes. The pressure drop, diffusion coefficients, and other parameters used in the simulation are listed in Appendix 2.

The structures that result from different glucose concentrations in the feed can be very different—for illustration purposes the results for a glucose feed concentration of 0.1 g/L (Fig. 3a and b) and 0.5 g/L (Fig. 4a and b) are presented. Figures 3a and 4a show the resulting structure and the corresponding concentrations in the reactor, while Figures 3b and 4b show some of the rates (growth, consumption, and production).

Some immediate observations can be done here:

- (1) Apparently the formation of islands of immobilized yeast allows for a better distribution of glucose, thus maximizing the production of the desired protein.
- (2) The effect of the glucose concentration can be seen as larger islands of cells for higher glucose concentrations. With higher glucose concentrations, the diffusion driving force into the islands is larger and thus allows for larger islands before the inner cells suffer from nutrient limitation.
- (3) The specific growth rate for glucose fermentation follows a similar pattern to the glucose distribution, whereas glucose oxidation was predominant in the regions where glucose is available in lower concentrations, and therefore, the respiratory metabolism is not subject to overflow metabolism in those regions.

- (4) A complementary pattern to the glucose distribution is obtained for the ethanol oxidation, which only takes place when glucose is depleted.

## Benchmarking

In order to assess the gains in protein concentration obtained by using structurally optimized reactors rather than reactors where the immobilized biomass is homogeneously distributed throughout the microbioreactor, the protein concentrations at the reactor outlet were determined for the spatially optimized reactors for different glucose feed concentrations (0.001 up to  $1 \text{ g L}^{-1}$ ). These concentrations were compared to the maximum protein concentrations obtained at the outlet, using the same glucose feed concentrations, where the immobilized yeast is homogeneously distributed at the optimal concentration. All the optimized reactors have an average cell concentration that is lower than that of the corresponding homogeneous reactor.

As illustrated in Table I, the protein mass flow rate at the outlet increased at least fivefold for all the simulated glucose feed concentrations when topology optimization was applied as opposed to the homogenous reactor. The increase in protein concentration at the outlet was more than eightfold for glucose feed concentrations between 0.005 and  $0.5 \text{ g L}^{-1}$ . In this range of concentrations, the significant gain in protein concentration can be explained by the fact that a structurally optimized distribution where flow is distributed and islands of biomass are surrounded by streams of liquid flow, allows for a balanced distribution of glucose across the reactor leading to higher local protein production rates.

## Conclusions and Outlook

This first investigation of the potential of topology optimization for improvement of microbial cultivation processes at microscale has clearly shown that the use of this

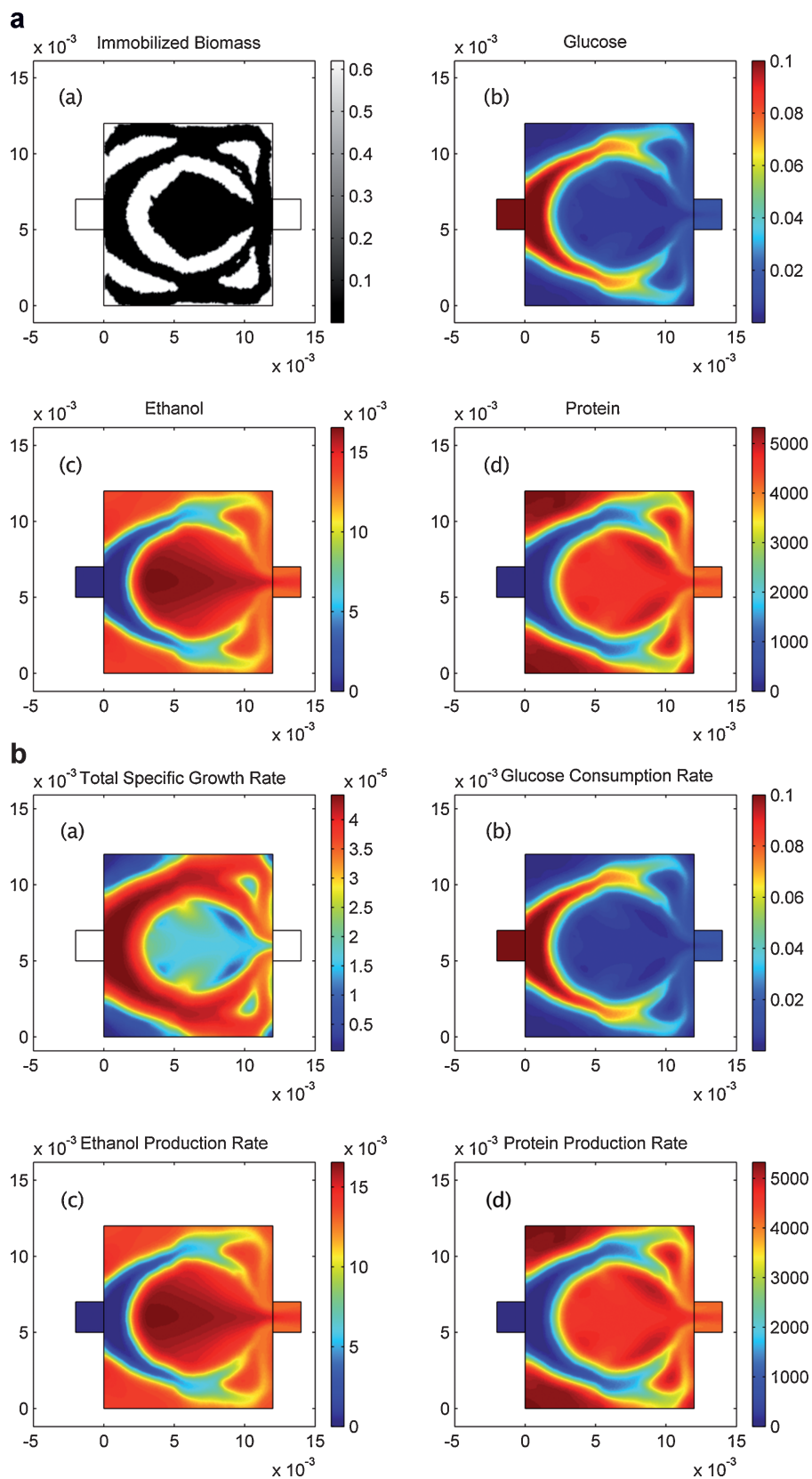


**Figure 3.** a: Resulting structure and concentrations for a glucose inflow concentration of  $0.1 \text{ g L}^{-1}$ . a: Distribution of biomass where white = cells and black = fluid, (b) glucose concentration [ $\text{g L}^{-1}$ ], (c) ethanol concentration [ $\text{g L}^{-1}$ ] and (d) protein concentration [ $\text{U L}^{-1}$ ]. b: Rates in the optimized design for a glucose flow concentration of  $0.1 \text{ g L}^{-1}$ . a: Total specific growth rate [ $\text{s}^{-1}$ ], (b) glucose consumption rate [ $\text{g (L s)}^{-1}$ ], (c) ethanol production rate [ $\text{g (L s)}^{-1}$ ], and (d) protein production rate [ $\text{U (L s)}^{-1}$ ].

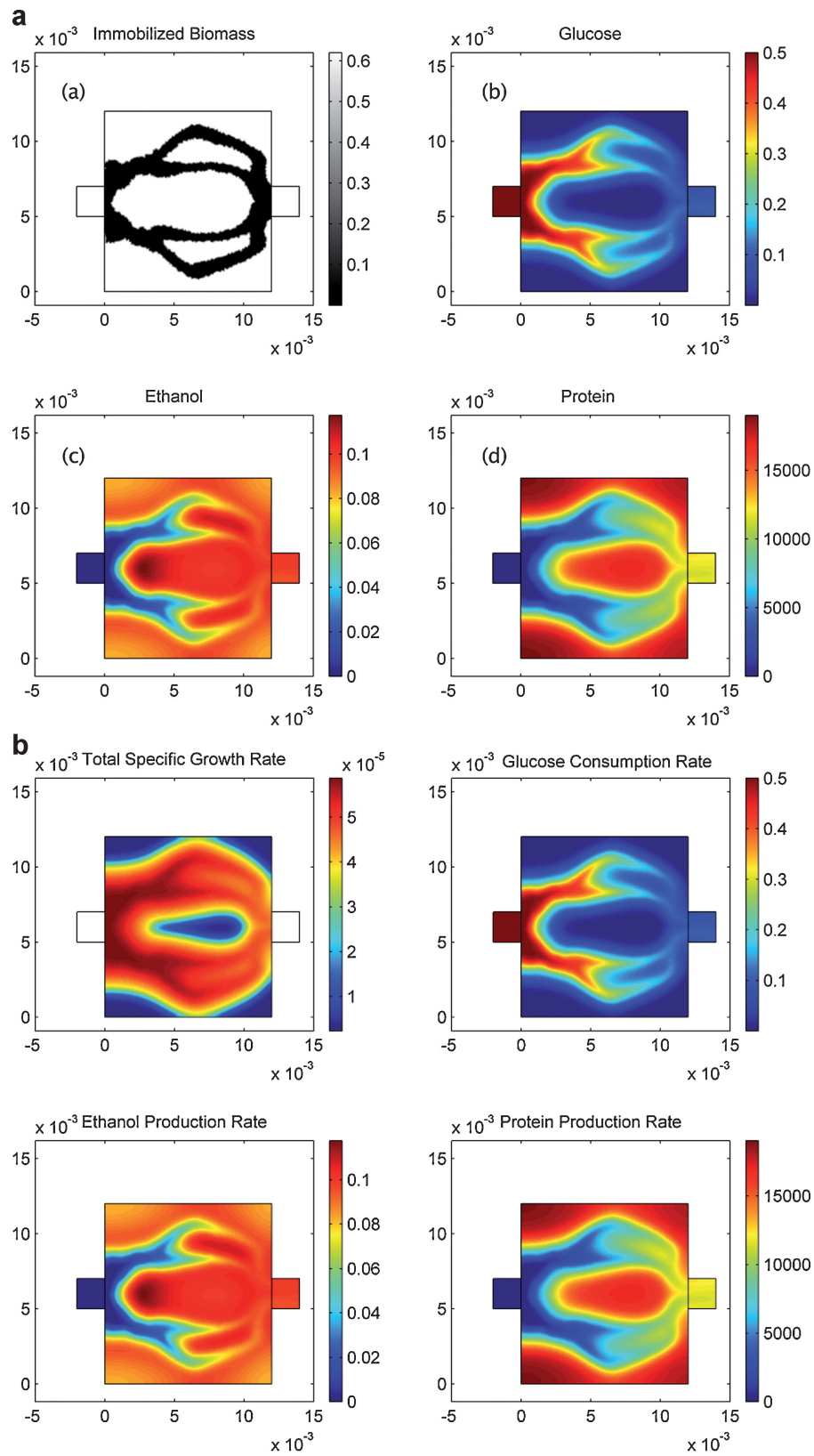


**Figure 4.** a: Resulting structure and concentrations for a glucose inflow concentration of  $0.5 \text{ g L}^{-1}$ . a: Distribution of biomass where white = cells and black = fluid, (b) glucose concentration [ $\text{g L}^{-1}$ ], (c) ethanol concentration [ $\text{g L}^{-1}$ ], and (d) protein concentration [ $\text{U L}^{-1}$ ]. b: Rates in the optimized design for a glucose flow concentration of  $0.5 \text{ g L}^{-1}$ . a: Total specific growth rate [ $\text{s}^{-1}$ ], (b) glucose consumption rate [ $\text{g (L s)}^{-1}$ ], (c) ethanol production rate [ $\text{g (L s)}^{-1}$ ], and (d) protein production rate [ $\text{U (L s)}^{-1}$ ].

**Table I.** Comparison of the total protein outputs for the homogeneous and the optimized reactor at different glucose feed concentrations.

Glucose feed conc. (mg L <sup>-1</sup> )	Protein flow at the reactor outlet (U s <sup>-1</sup> )		
	Homogeneous reactor	Structurally optimized reactor	Increase (fold)
1	0.3	2.7	5.8
5	1.4	12.9	9.1
10	2.7	23.1	8.4
30	7.2	57.4	8.0
50	10.7	91.7	8.5
100	17.6	170.3	9.7
200	25.2	229.5	9.1
500	39.0	325.2	8.3
1,000	63.8	380.4	6.0

methodology can potentially lead to microreactors with a significantly higher productivity than conventional reactor designs where immobilized biomass is homogeneously distributed. If we assume that results can be extrapolated to larger scales, topology optimization thus holds the promise of significant increase in the productivity compared to existing stirred tanks. However, it also poses a number of questions and areas for further investigation as discussed below.

In this study we focused on one single strain under specific operating conditions. It would be very interesting to see if the general results also hold for other cell types, for example, mammalian cells or filamentous fungi. Another interesting question is the shape of the reactor itself. We considered here a very simple rectangular reactor with one inflow and one outflow. Is a rectangle the best shape? Or might a design with several in- and outflows perform even better? In this respect, if substrate inhibition is a major issue for a reaction of interest, one should expect that a microreactor design with several inflows of substrate along the length of the reactor would be the best solution.

The question of practical applicability is of utmost importance. To perform an experimental validation of the simulation outcome the necessary techniques to transfer these theoretical results into the laboratory have to be established first. The fabrication of the sponge-like structure and inoculation of the structure with cells has been demonstrated (Akay et al., 2004; Karagöz et al., 2008). Now this work has to be repeated using the optimized structures. Then, a comparison between the effective cultivations and the corresponding simulations has to be done in order to prove that the simulations can reliably predict laboratory results.

In this study we have assumed that aeration is sufficient and have not modeled the possible effects of variations in oxygen concentration. Adding this variable into the simulation is possible as it basically adds another diffusion term. In practice bubbleless aeration via the top/bottom of the reactor could be a suitable solution for oxygen supply, a technique that has been used widely in microreactor designs (Lee et al., 2006; Schäpper et al., 2010; Zhang et al., 2005). If one assumes, as in this model, that the reactor

height is only a few tens of micrometers, and that, for example, both the floor and the ceiling of the reactor consisted of a membrane for bubbleless aeration, then it might well be possible to supply sufficient oxygen to the cells. Other models available in the literature could be considered instead, if one wishes to model oxygen availability (e.g., Sonnleitner and Käppli, 1986).

Once the issue of practicability has been addressed, then the issue of scaling-up becomes relevant when laboratory results have to be transferred to pilot or production scale. Which strategy (scaling-out or scaling-up) should be followed? For scaling-up, which parameter can be used for comparison purposes? For conventional CSTR type reactors, Islam et al. (2008) showed that the oxygen transfer coefficient ( $k_L a$ ) is a good criterion for translation between different scales. However, this might well not be the correct parameter for the kind of reactors presented here. It might just as well be the density of cells or the laminarity of the flow. Finding the correct translation criterion is a challenge in itself.

Whilst the results presented here show that topology optimization can lead to significantly higher productivities in a theoretical setting, the methodology will have to be applied to relevant industrial problems which justify the additional effort in moving from the laboratory to industrial settings. For example, the results show that the methodology is especially interesting for low concentrations of glucose in the feed as this enhances the need for an optimal distribution of nutrients. Even more interesting examples would, for example, be those where the substrate or the product is highly toxic to the cells as this would further encourage an optimal distribution of cells.

## Nomenclature

$\alpha(r)$	Darcy friction coefficient (Pa s m <sup>-2</sup> )
$\eta$	viscosity (Pa s)
$\gamma$	set of design variables
$\Omega$	design region
$\Phi$	objective function
$\vec{r}$	position coordinate vector (m)
$\vec{u}$	flow velocity (m s <sup>-1</sup> )
$D_A$	diffusion coefficient for A (m <sup>2</sup> s <sup>-1</sup> )
E	ethanol concentration (g L <sup>-1</sup> )
G	glucose concentration (g L <sup>-1</sup> )
$p$	pressure (Pa)
P	product/protein concentration (U L <sup>-1</sup> )
R	rate of formation (U (L s) <sup>-1</sup> )
$X_f$	total free (suspended) biomass (g L <sup>-1</sup> )
$X_f^+$	plasmid bearing freely suspended biomass (g L <sup>-1</sup> )
$X_{im}$	immobilized cells (g <sub>cells</sub> g <sub>carrier</sub> <sup>-1</sup> )
$X_{im}^+$	immobilized cells with plasmid (g <sub>cells</sub> g <sub>carrier</sub> <sup>-1</sup> )

The PhD project of Daniel Schäpper is funded by Novozymes A/S and the Technical University of Denmark (DTU) through a Novozymes Bioprocess Academy PhD stipend. Fridolin Okkels is funded by the Danish Agency for Science, Technology and Innovation (grant no. 09-065029).

## Appendix 1

The model used within the topology optimization routine is presented below. It was implemented and solved using the commercial software COMSOL. A list of parameters and corresponding values is given in Table A1.

The total immobilized biomass ( $X_{\text{im}}$ ) is the actuator variable. It is defined based on a design parameter,  $\gamma$ , that will be varied in the routine iterations.  $(1 - \gamma)$  represents the fraction of carrier used by the immobilized biomass (Eq. A.1).

$$X_{\text{im}} = (1 - \gamma)X_{\text{im}}^{\text{max}} \quad (\text{A.1})$$

The plasmid bearing immobilized biomass, that is, the fraction of immobilized biomass that possesses the genetic information necessary to the production of the desired protein, can be determined by multiplying the total immobilized biomass by the plasmid loss factor  $p$ , thus implying a constant factor of plasmid loss (Eq. A.2).

$$X_{\text{im}}^+ = (1 - p)X_{\text{im}} \quad (\text{A.2})$$

The transport of the suspended (free) biomass, glucose, and ethanol is carried out by fluid convection and diffusion, and is mathematically described by the Equations (A.3)–(A.6), where  $X_{\text{im}}^{\text{act}}/(X_{\text{im}}^{\text{act}} + X_{\text{im}})$  accounts for the fact that not all immobilized cells are actively growing

$$\begin{aligned} \bar{u}\nabla X_f = & (\mu_1 + \mu_2 + \mu_3) \left[ \frac{X_{\text{im}}^{\text{act}}}{X_{\text{im}}^{\text{act}} + X_{\text{im}}} \frac{X_{\text{im}} P_c}{V_r} + X_f \right] \\ & + D_{X_f} \nabla^2 X_f \end{aligned} \quad (\text{A.3})$$

$$\begin{aligned} \bar{u}\nabla X_f^+ = & (\mu_1 + \mu_2 + \mu_3) \left[ \frac{X_{\text{im}}^{\text{act}}}{X_{\text{im}}^{\text{act}} + X_{\text{im}}^+} \frac{X_{\text{im}}^+ P_c}{V_r} + X_f^+ \right] \\ & + D_{X_f^+} \nabla^2 X_f^+ \end{aligned} \quad (\text{A.4})$$

$$\begin{aligned} \bar{u}\nabla G = & - \left[ \frac{\mu_1}{Y_{X/G}^F} + \frac{\mu_2}{Y_{X/G}^O} \right] \left[ \frac{X_{\text{im}}^{\text{act}}}{X_{\text{im}}^{\text{act}} + X_{\text{im}}} \frac{X_{\text{im}} P_c}{V_r} + X_f \right] \\ & + D_G \nabla^2 G \end{aligned} \quad (\text{A.5})$$

$$\begin{aligned} \bar{u}\nabla E = & \left[ Y_{E/X} \mu_1 - \frac{\mu_3}{Y_{X/E}^O} \right] \left[ \frac{X_{\text{im}}^{\text{act}}}{X_{\text{im}}^{\text{act}} + X_{\text{im}}} \frac{X_{\text{im}} P_c}{V} + X_f \right] \\ & + D_E \nabla^2 E \end{aligned} \quad (\text{A.6})$$

The growth rates for each of the pathways (Eqs. A.7–A.9) consist of modified Monod equations where  $K_{i'}$  and  $k_{i'}$  are saturation and regulation constants which have been recalculated in order to obtain explicitly defined functions which are mathematically equivalent to the implicitly defined expressions proposed in the work of Zhang et al. (1997).  $k_{i'}$  in Equations (A.7) and (A.8) have no physical meaning. The term  $(1 - \tanh(G))$  in Equation (A.9) operates as switch function that tends to 0 when the glucose (G) concentration is high and to 1 when G approaches zero.

$$\mu_1 = \mu_{1,\text{max}} \frac{G}{K_{1'} + G} \frac{1 + k_{a'} G}{k_{a'} G} \quad (\text{A.7})$$

**Table A1.** List of model parameters.

Parameter	Description	Value	Unit
$X_{\text{im}}^{\text{act}}$	Fraction of active immobilized cells (Brányik et al., 2004)	0.62	$\text{g}_{X_{\text{im}}} \text{g}_{\text{C}}^{-1}$
$P_c/V_r$	Carrier mass/reactor volume (Brányik et al., 2004)	13.6	$\text{g L}^{-1}$
$p$	Plasmid loss factor (Zhang et al., 1997)	0.05	—
$Y_{X/G}^F$	Yield coefficient of biomass on glucose for glucose fermentation (Zhang et al., 1997)	0.12	$\text{g}_X \text{g}_G^{-1}$
$Y_{X/G}^O$	Yield coefficient of biomass on glucose for glucose oxidation (Zhang et al., 1997)	0.48	$\text{g}_X \text{g}_G^{-1}$
$Y_{E/X}$	Yield coefficient of ethanol on biomass for glucose fermentation (Zhang et al., 1997)	3.35	$\text{g}_E \text{g}_X^{-1}$
$Y_{X/E}$	Yield coefficient of biomass on ethanol for ethanol oxidation (Zhang et al., 1997)	0.65	$\text{g}_X \text{g}_E^{-1}$
$\alpha_2$	Protein yield coefficient for glucose oxidation (Zhang et al., 1997)	32.97	$\text{U g}_X^{-1}$
$\alpha_3$	Protein yield coefficient for ethanol oxidation (Zhang et al., 1997)	33.80	$\text{U g}_X^{-1}$
$\mu_{1,\text{max}}$	Maximum specific growth rate for glucose fermentation (Zhang et al., 1997)	0.38	$\text{L h}^{-1}$
$\mu_{2,\text{max}}$	Maximum specific growth rate for glucose oxidation (Zhang et al., 1997)	0.25	$\text{L h}^{-1}$
$\mu_{3,\text{max}}$	Maximum specific growth rate for ethanol oxidation (Zhang et al., 1997)	0.10	$\text{L h}^{-1}$
$K_{1'}$	Saturation constant	$1.8 \times 10^{-1}$	$\text{g L}^{-1}$
$K_{2'}$	Saturation constant	$10^{-2}$	$\text{g L}^{-1}$
$k_{a'}$	Enzyme pool regulation constant	$-4.0 \times 10^{-3}$	—
$k_{b'}$	Enzyme pool regulation constant	2.3	—
$k_{c'}$	Enzyme pool regulation constant	20	—
$k_{d'}$	Enzyme pool regulation constant	2.9	—

$$\mu_2 = \mu_{2,\max} \frac{G}{K_2' + G} \frac{1 + k_c'G}{1 + k_c'k_d'G} \quad (\text{A.8})$$

$$\mu_3 = \mu_{3,\max} \frac{E}{K_3 + E} (1 - \tanh(G)) \quad (\text{A.9})$$

In a topology optimization routine, the optimization function is, by default, minimized. As in the case of the presented work, it is desired that the protein product rate (Eq. A.10) is maximized rather than minimized, a negative signal is added when writing the optimization function  $\Phi$  (Eq. A.11)

$$R_p = (\alpha_2\mu_2 - \alpha_3\mu_3) \left[ \frac{X_{\text{im}}^+ P_c}{V_r} + X_f^+ \right] \quad (\text{A.10})$$

$$\Phi(\gamma) = - \int_{\Omega} R_p(t) dV \quad (\text{A.11})$$

## Appendix 2

Simulation parameters are shown in Table AII.

**Table AII.** Simulation parameters.

Parameter	Description	Value	Unit
$dp$	Pressure drop	0.1	Pa
$D_{X_{f+}}$	Diffusion coefficient	$1 \times 10^{-10}$	$\text{m}^2 \text{s}^{-1}$
$D_G$	Diffusion coefficient for glucose	$1 \times 10^{-9}$	$\text{m}^2 \text{s}^{-1}$
$D_E$	Diffusion coefficient for ethanol	$1 \times 10^{-9}$	$\text{m}^2 \text{s}^{-1}$
$D_P$	Diffusion coefficient for the product	$1 \times 10^{-9}$	$\text{m}^2 \text{s}^{-1}$
$l$	Reactor length	$1.2 \times 10^{-2}$	m
$w$	Reactor width	$1.2 \times 10^{-2}$	m
$h$	Reactor height	$1 \times 10^{-3}$	m
$\eta$	Fluid viscosity	$1 \times 10^{-3}$	Pa s
$G_{\text{inlet}}$	Glucose feed concentration	$1 \times 10^{-3} - 1$	$\text{g L}^{-1}$

The diffusion coefficient for the suspended biomass (cells) can be estimated by the Einstein-relation for diffusion,  $D = k_B T / (6\pi a \eta)$ , where  $a$  is the radius of the cells and  $k_B$  is Boltzmann's constant. This estimates a coefficient of  $4.4 \times 10^{-14} \text{ m}^2 \text{ s}^{-1}$  ( $a = 5 \mu\text{m}$ ,  $T = 300 \text{ K}$ ). However, very small diffusion coefficients may result in very steep concentration gradients, and for the numerical optimization method to resolve these gradients, a lot of computer memory is needed. As a consequence, we have had to increase the diffusion coefficient  $D_{X_{f+}}$  to  $10^{-10} \text{ m}^2 \text{ s}^{-1}$  and  $D_E = D_G = D_P = 10^{-9} \text{ m}^2 \text{ s}^{-1}$  for the optimization to be doable.

## References

Akay G, Erhan E, Keskinler B. 2004. Bioprocess intensification in flow-through monolithic microbioreactors with immobilized bacteria. *Biotech Bioeng* 90(2): 180–190.

Bendsøe MP, Kikuchi N. 1988. Generating optimal topologies in structural design using a homogenization method. *Comput Method Appl M* 71: 197–224.

Bendsøe MP, Sigmund O. 2002. *Topology optimization—Theory, methods and applications*, 2nd edn. Berlin, Heidelberg: Springer.

Bendsøe MP, Lund E, Olhoff N, Sigmund O. 2005. Topology optimization—Broadening the areas of application. *Control Cybern* 34:7–35.

Borrvall T, Petersson J. 2003. Topology optimization of fluids in Stokes flow. *Int J Numer Meth Fluids* 41:77–107.

Brányik T, Vicente AA, Kuncová G, Podrazky O, Dostálek P, Teixeira J. 2004. Growth model and metabolic activity of brewing yeast biofilm on the surface of spent grains: A biocatalyst for continuous beer fermentation. *Biotechnol Prog* 20:1733–1740.

Desmet G, De Greef J, Verelst H, Baron GV. 2003. Performance limits of isothermal packed bed and perforated monolithic bed reactors operated under laminar flow conditions. I. General optimization analysis. *Chem Eng Sci* 58:3187–3202.

Enfors SO, Jahic M, Rozkov A, Xu B, Hecker M, Jürgen B, Krüger E, Schweder T, Hamer G, O'Beirne D, Noisommit-Rizzi N, Reuss M, Boone L, Hewitt C, McFarlane C, Nienow A, Kovacs T, Trägårdh C, Fuchs L, Revstedt J, Friberg PC, Hjertager B, Blomsten G, Skogman H, Hjort S, Hoeks F, Lin HY, Neubauer P, van der Lans R, Luyben K, Vrabel P, Manelius Å. 2001. Physiological responses to mixing in large scale bioreactors. *J Biotechnol* 85:175–185.

Eschenauer HA, Olhoff N. 2001. Topology optimization of continuum structures: A review. *Appl Mech Rev* 54:331–390.

Gernaey KV, Eliasson Lantz A, Tuvesson P, Woodley J, Sin G. 2010. Application of mechanistic models to fermentation and biocatalysis for next generation processes. *Trends Biotechnol* 28:346–354.

Gregersen MM, Okkels F, Bazant MZ, Bruus H. 2009. Topology and shape optimization of induced-charge electro-osmotic micropumps. *New J Phys* 11:075019.

Højgaard-Olesen L, Okkels F, Bruus H. 2006. A high-level programming-language implementation of topology optimization applied to steady-state Navier-Stokes flow. *Int J Numer Methods Eng* 65:975–1001.

Islam R, Tisi D, Levy M, Lye G. 2008. Scale-up of *Escherichia coli* growth and recombinant protein expression conditions from microwell to laboratory and pilot scale based on matched  $k_L a$ . *Biotechnol Bioeng* 99:1128–1139.

Karagöz P, Erhan E, Keskinler B, Özkan M. 2008. The use of microporous divinyl benzene copolymer for yeast cell immobilization and ethanol production in packed-bed reactor. *Appl Biochem Biotech* 152(1): 66–73.

Lapin A, Müller D, Reuss M. 2004. Dynamic behavior of microbial populations in stirred bioreactors simulated with Euler-Lagrange methods: Traveling along the lifelines of single cells. *Ind Eng Chem Res* 43:4647–4656.

Lee HLT, Boccazzi P, Ram RJ, Sinskey AJ. 2006. Microbioreactor arrays with integrated mixers and fluid injectors for high-throughput experimentation with pH and dissolved oxygen control. *Lab Chip* 6:1229–1235.

Müller S, Harms H, Bley T. 2010. Origin and analysis of microbial population heterogeneity in bioprocesses. *Curr Opin Biotech* 21:100–113.

Okkels F, Bruus H. 2007a. Scaling behavior of optimally structured catalytic microfluidic reactors. *Phys Rev E* 75(1): 016301.

Okkels F, Bruus H. 2007b. Design of micro-fluidic bio-reactors using topology optimization. *J Comput Theor Nanosci* 4(4): 814–816.

Schäpper D, Alam MNHZ, Szita N, Eliasson Lantz A, Gernaey KV. 2009. Application of microbioreactors in fermentation process development: A review. *Anal Bioanal Chem* 395:679–695.

Schäpper D, Stocks S, Szita N, Eliasson Lantz A, Gernaey KV. 2010. Development of a single-use microbioreactor for cultivation of microorganisms. *Chem Eng J* 160:891–898.

Sonnleitner B, Käppli O. 1986. Growth of *Saccharomyces cerevisiae* is controlled by its limited respiratory capacity: Formulation and verification of a hypothesis. *Biotechnol Bioeng* 28:927–937.

Szita N, Zhang Z, Boyle P, Sinskey AJ, Jensen KF. 2005. Development of a multiplexed microbioreactor system for high-throughput bioprocessing. *Lab Chip* 5(8): 819–826.

Zhang Z, Scharer JM, Moo-Young M. 1997. Mathematical model for aerobic culture of a recombinant yeast. *Bioprocess Eng* 17:235–240.

Zhang Z, Szita N, Boccazzi P, Sinskey AJ, Jensen KF. 2005. A well-mixed, polymer-based microbioreactor with integrated optical measurements. *Biotechnol Bioeng* 93(2): 286–296.

Zhang Z, Perozziello G, Boccazzi P, Sinskey AJ, Geschke O, Jensen KF. 2007. Microbioreactors for bioprocess development. *JALA* 12:143–151.